

# Probabilistic estimation of floor response spectra in masonry infilled reinforced concrete building portfolio

Daniele Perrone<sup>a,\*</sup>, Emanuele Brunesi<sup>b</sup>, Andre Filiatrault<sup>c</sup>, Roberto Nascimbene<sup>b</sup>

<sup>a</sup> School of Advanced Studies IUSS Pavia, Italy

<sup>b</sup> European Centre for Training and Research in Earthquake Engineering, Italy

<sup>c</sup> School of Advanced Studies IUSS Pavia, Italy & State University of New York at Buffalo, USA

## ARTICLE INFO

### Keywords:

Floor response spectra  
Non-structural elements  
Masonry infills  
Seismic demand  
Regional risk models

## ABSTRACT

The seismic performance of non-structural elements is now recognized to be a key issue in the seismic assessment and earthquake related loss estimation of buildings, both at the individual and regional scale. The evaluation of the seismic demand on non-structural elements in many modern building codes is often based on inaccurate distributions of floor accelerations. For this reason, some design oriented simplified methodologies have been developed recently to predict floor response spectra in reinforced concrete buildings. Although the influence of masonry infills on the seismic performance of reinforced concrete buildings has been widely demonstrated, infills are generally neglected both in the design and in the evaluation of floor response spectra, which could lead to un-conservative design of non-structural elements. In this paper, the effect of masonry infills on absolute acceleration and relative displacement floor response spectra for reinforced concrete buildings subjected to frequent (serviceability level) earthquakes is investigated through a probabilistic framework. A database of one hundred masonry infilled reinforced concrete frames, representative of the European context, was generated and each building analyzed through nonlinear time history analyses. From the results of these analyses, the acceleration and displacement response spectra at different floor levels of both bare and infilled frame archetypes were then computed. The effectiveness of the most common assumptions made in regional risk models to estimate the non-structural losses is investigated and a first attempt at a more refined approach taking into account the effect of masonry infills is proposed.

## 1. Introduction

Reconnaissance reports and surveys carried out during recent earthquakes, as well as advanced numerical loss estimation studies, indicated repetitively that a significant part of the observed earthquake related losses can be attributed to damage to non-structural elements [1,2]. Non-structural elements represent all the systems and elements attached to the floors and walls of a building that are not part of the vertical and lateral load-bearing structural systems [3], but that are subjected to the same dynamic excitation during a seismic event. As reported by Miranda and Taghavi [4], non-structural elements represent most of the total investments in typical buildings. In hospital buildings, for example, the structures make up approximately only 8% of the total monetary investments [4]. At the same time, the damage to non-structural elements not only result in major economic losses but could also represent a threat to life. Due to the numerous typologies of non-structural elements installed in buildings, their vulnerability could

significantly affect the immediate functionality of buildings because they generally exhibit damage at low (serviceability) seismic intensities, when the supporting structures respond mainly in the elastic range. This issue is paramount for strategic facilities, such as hospitals and schools that should remain operational in the post-earthquake emergency response phase.

An example of the importance of non-structural elements on the post-earthquake functionality of critical facilities was observed during the recent 2010 Chile earthquake. Following this seismic event, four hospitals completely lost their functionality and over 10 more lost 75% of their functionality due to damage to sprinkler piping systems [5]. Significant non-structural damage was also observed in Italy during the 2009 L'Aquila earthquake and the 2012 Emilia earthquake, as well as during the 2016 Amatrice earthquake [1,6,7]. The most common non-structural element failures, observed during these recent seismic events, were related to partition walls experiencing large in-plane story drifts and to damage to storage rack systems and ceiling systems [1,8].

\* Corresponding author.

E-mail address: [daniele.perrone@iusspavia.it](mailto:daniele.perrone@iusspavia.it) (D. Perrone).

In the light of these considerations, the seismic performance of non-structural elements is now recognized to be a key issue in performance-based earthquake engineering to ensure a desired building system performance for a given intensity of seismic excitation [9]. The FEMA P-58 methodology [10] for the seismic performance assessment of buildings considers the contributions of non-structural elements to the expected losses by: (1) identifying the non-structural elements in the building, (2) developing probabilistic relationships between damage states and engineering demand parameters (fragility curves), (3) identifying the damage to non-structural elements, and (4) evaluating the consequences of the predicted damage in terms of hazard to occupants, cost of repair, and downtime. The seismic demand on the non-structural elements is obtained by recording the maximum inter-story drifts and the peak floor accelerations from multi-strips nonlinear time history analyses. The FEMA P-58 methodology represents a powerful tool to assess the performance of single buildings but it is not so easily feasible for building portfolios due to its complexity and computational effort. Because of this, the HAZUS methodology is one of the most widespread methods for seismic loss estimation at the regional scale [11]. HAZUS allows analysts to estimate the expected annual losses of a building portfolio through a simplified approach similar to the capacity spectrum method. Although the HAZUS methodology is simple, some assumptions on the evaluation of the non-structural damage state probabilities have been questioned [11].

In regional scale seismic risk models, non-structural elements are generally classified as acceleration-sensitive or drift-sensitive, based on the main engineering demand parameter affecting their response. Partition walls and glazing systems are examples of non-structural elements vulnerable to story drifts induced in buildings. On the other hand, suspended ceilings, bookshelves, light fixtures, piping systems, and rigidly attached elements are examples of acceleration-sensitive non-structural elements. In order to assess the performance of drift-sensitive non-structural elements, the response of the structure in terms of inter-story drifts is required, while for acceleration-sensitive non-structural elements, the absolute acceleration floor response spectra (FRS) need to be evaluated.

Starting from the questionable suitability of code prescriptions and code-compliant guidelines [12,13], some authors proposed simplified methodologies to predict absolute acceleration FRS for elastic and inelastic single-degree-of-freedom (SDOF) and multi-degree-of-freedom (MDOF) systems [14–19]. Petrone *et al.* [14] and Vukobratovic and Fajfar [15] proposed two different methods to evaluate FRS for MDOF structures. The methodology proposed by Petrone *et al.* [14] is focused on European buildings designed according to Eurocode 8 [12] prescriptions and subjected to frequent (serviceability level) earthquake ground motions. The approach proposed by Vukobratovic and Fajfar [15] was calibrated both for elastic and inelastic supporting structures. The authors highlighted the significant influence of higher modes on FRS. Similar considerations have been introduced in the methodology developed recently by Sullivan *et al.* [16]. This simple approach was originally proposed for linear and nonlinear SDOF structures and was recently extended to linear and nonlinear MDOF systems [17,19].

Recently, a methodology was also developed by Calvi [20] to evaluate relative-displacement FRS. This methodology is a powerful tool to evaluate the seismic displacements of non-structural elements relative to their attachment points, which are typically required by seismic provisions but without providing any guidance on how to do so. Relative-displacement FRS also define the seismic demand in the direct displacement-based seismic design framework for ductile non-structural elements recently proposed by Filiatrault *et al.* [21].

Note that the methodologies currently available in the literature to evaluate FRS have been mainly developed and validated for reinforced concrete (RC) framed buildings, studied in a deterministic fashion, without considering the influence of masonry infills, which are generally present in these structures. As reported by many authors, the masonry infills significantly affect the seismic response of RC moment-

resisting frames and consequently the evaluation of FRS. Severe in-plane (IP) and out-of-plane (OOP) damage to unreinforced masonry infills was often observed during past earthquakes. To address this issue, experimental and analytical studies on IP and OOP behaviour of unreinforced masonry infills were carried out in the last years [22–25]. At the same time, it is worth noting that the methodologies currently available in the literature require the knowledge of the elastic dynamic response of the analyzed buildings. For this reason, these methods are not feasible for regional scale applications and, to the authors' knowledge, there are no simplified methodologies that exist to evaluate FRS in masonry infilled RC moment resisting structures to be used in regional scale risk models. In light of this, one of the main objectives of this study is to propose seismic demand models that could be used to predict the median floor spectral accelerations in RC moment resisting frames with and without masonry infills.

## 2. Motivation and scope of the study

At the regional scale, the main efforts are generally devoted at developing specific frameworks to produce seismic physical vulnerability models of different building typologies [26,27], but the non-structural losses are still often neglected. When non-structural elements are considered, sweeping assumptions are usually made both for the definition of the fragility functions as well as of the seismic demands [12]; these assumptions could yield major inaccuracies that could affect significantly the cost/benefit analysis results. Another shortcoming is that probabilistic floor seismic demand models to be implemented in regional risk models are not yet available in the literature for any building typology, and this significantly reduces the prediction capabilities of regional risk models due to the inaccuracy of the non-structural damage state probability evaluation.

As previously discussed, some simplified methods are available in the literature to predict the FRS of reinforced concrete buildings [14–17], but the influence of masonry infills, which are usually present in these structures, was not considered in any of them. The effect of masonry infills has been widely studied in the literature, both from the experimental [28–31] and numerical [32,33] points of view. The IP-OOP interaction has been recently studied for the analysis of the seismic response of 3D RC buildings. In particular, based on the results of experimental studies, numerical models able to predict the reduction of the OOP capacity due to the IP damage have been developed [24–25]. However, few studies have investigated the influence of masonry infills on FRS in RC buildings [34,20]. For instance, Lucchini *et al.* [33] investigated the influence of masonry infills and damping models on FRS in nonlinear buildings. It was found that the infill walls can significantly affect the floor acceleration peak profile, at a given intensity, as well as the ordinates of the FRS at all stories. More recently, Surana *et al.* [35] studied the effect of unreinforced masonry infills on the inelastic FRS of RC frame buildings. These results lay evident that the influence of masonry infills cannot be neglected in the evaluation of FRS in RC frames, particularly for frequent earthquakes, in which the initial stiffness of the infills is not drastically affected by the cracking developing in the masonry.

Based on these considerations, floor response spectra in masonry infilled RC frames subjected to frequent (serviceability level) earthquakes is investigated in this study through a probabilistic framework. One hundred masonry infilled RC frames were randomly generated, through a Monte Carlo simulation, considering the geometric and mechanical properties of typical European buildings. Each RC frame was then designed according to Eurocode 8 [12] seismic provisions for a medium-to-high seismicity site in Italy. The building-to-building and the record-to-record variabilities were considered in order to investigate the influence of the masonry infills on the FRS and to provide preliminary data for proposing a possible approach that can be implemented to improve the prediction capability of regional risk models in terms of non-structural losses. Because the non-structural elements

mainly affect the expected losses for moderate seismic intensities, a short return period (70 years) of ground motions at the buildings site was considered in this study.

In regional scale loss estimation studies, many assumptions are considered in order to minimize the computational efforts. Once a probabilistic seismic hazard analysis for the region of interest is performed, the definition of a building taxonomy allows to identify the building typologies that characterize the region. For each building typology, analysts are required to define fragility functions that describe the likelihood of reaching, or exceeding, particular damage states, given an estimate of peak building response. In the definition of the fragility functions the variability in terms of design approaches, geometrical properties and structural typologies is generally considered. This procedure allows to account for the variability due to the hazard and structural fragility. In the evaluation of the expected losses related to the non-structural elements, if considered, much more simplifications are considered. The fragility functions are generally only defined based on the typology of non-structural elements (acceleration-sensitive and drift-sensitive) while the seismic demand is a function of the ground response spectrum. To overcome this shortcoming, the present study is also aimed at defining a more accurate seismic demand model to calculate the non-structural losses in regional scale risk models. Therefore, the proposed model (i) falls within the framework of the HAZUS methodology [11], (ii) is meant to predict the median value of the floor spectral acceleration in bare and infilled RC moment resisting frames, and (iii) results from probabilistic structural analyses (of the considered building portfolio), where non-structural elements other than infills are not included in the building models, as they do not affect the dynamic behaviour of the randomly sampled building realisations. The proposed seismic demand model takes into account not only the record-to-record variability but also the variability due to the dynamic properties of the building typology, in this case RC moment resisting frames (with and without masonry infills). In order to provide a better estimate of the non-structural losses, a similar procedure should be followed for each building typology in the building taxonomy. The adoption of this methodology could significantly improve the prediction of the likelihood of reaching, or exceeding, specific non-structural damage states, which would lead to a better definition of the seismic losses at regional scale.

### 3. Methodology

The influence of masonry infills on FRS was investigated by performing nonlinear time history analyses (NLTHAs) on a building population composed by one hundred RC moment resisting frames. A series of random variables (RVs) were selected, as described in the next section, to construct the building population. Fig. 1 reports the framework used for the evaluation of the FRS. Once the numerical modeling techniques were chosen, a Monte Carlo simulation was carried out to generate the building population based on the selected RVs. Simulated designs were undertaken and a planar numerical model of each building archetype was then developed. Finally, NLTHAs were performed in order to obtain acceleration and displacement time histories for different floors of interest, leading to the calculation of FRS for each floor of each building. Statistically representative FRS could then be used in regional scale non-structural loss evaluation. Note that the ensemble of ground motions was selected to be representative of a medium-high seismic zone in Italy for a probability of exceedance of 50% in 50 years, corresponding to an average return period equal to 70 years. In the next sections, the building population, the modelling approach as well as the ground motions selection are discussed in detail.

#### 3.1. Building population

A database of one hundred RC frames was randomly generated

using a Monte Carlo simulation. The RVs were selected following two criteria: (1) the threshold values and distributions associated with RVs are meant to be representative of the typical geometrical and mechanical characteristics of Italian buildings, (2) the randomly selected properties of the building archetypes were chosen considering only the parameters that mostly drive the dynamic behavior/response of infilled RC frames [28,36], whereas the other building parameters were treated as either deterministic or deterministic transformation of RVs. The influence of the variability in the geometrical and mechanical properties of the masonry infills were not considered because the main objective of the study is to quantify how the introduction of masonry infills in the model could affect the floor response spectra. RVs were assumed and treated as described below:

- Building height: the structure height was varied by varying both the number of stories and the inter-story height. The number of stories was varied between two and six. This choice is based on the typical number of stories observed in the Italy and Europe for RC building [37]. Previous studies underlined that the influence of the masonry infills on building response varies when increasing the number of stories; in particular, for building with more than six stories, the influence remain constant without further variation [36]. Based on this consideration, the number of stories was limited to six. The inter-story height was also varied by randomly selecting 2.75 m, 3.00 m and 3.25 m, with each height assumed to have the same probability of occurrence in the building population. This choice reflects the fact that the inter-story height does not vary significantly and is usually the minimum allowed by construction standards [38].
- Bay number and length: the number of bays was varied between three and six. Previous probabilistic studies dealing with fragility analysis for RC framed buildings assumed four bays as mean value [38,39]. In this study, it was decided to include the bay number as a RV because of the presence of the masonry infills. Amanat *et al.* [36] pointed out that the effect of the masonry infills is reduced when the number of bays increases, due to the higher stiffness of the bare frame. The beam span was assumed to be constant for all bays, and the bay length was varied between 3 and 6 m, according to previous studies available in the literature [39,40].
- Design loads: the dead loads were kept constant for all RC frames assuming a weight of the slab equal to 3.25 kN/m<sup>2</sup> and assuming a tributary area of 5 m. On the other hand, the live loads were considered as a RV, by varying them between 2 kN/m<sup>2</sup> and 4 kN/m<sup>2</sup> to simulate different building uses.
- Material properties: the unconfined concrete compressive stress was randomly chosen between 25 and 40 MPa, while the characteristic yielding rebar strength was randomly selected between 375 and 430 MPa. The mechanical properties of the masonry infills were based on the observations by Sassun *et al.* [29] and De Luca *et al.* [30] who pointed out that the clay hollow masonry is the most widespread masonry typology used for masonry infill panels and, for this reason, it was selected in this study. The mechanical properties of the infill panels were chosen based on the study proposed by Cavalieri and Di Trapani [28]. In particular, the vertical and horizontal Young's moduli were taken equal to 6401 and 5038 MPa, respectively, while the compressive and shear strength were taken equal to 8.66 MPa and 1.07 MPa, respectively.

The frames were designed according to the Eurocode 8 seismic provisions assuming a force reduction factor  $q = 3.75$ , corresponding to a ductility class B. A firm ground site near the city of Cassino (Italy), characterized by a design peak ground acceleration (with a return period of 475 years) of 0.21 g, was selected.

#### 3.2. Modelling approach

For each RC frame, a detailed planar numerical model was

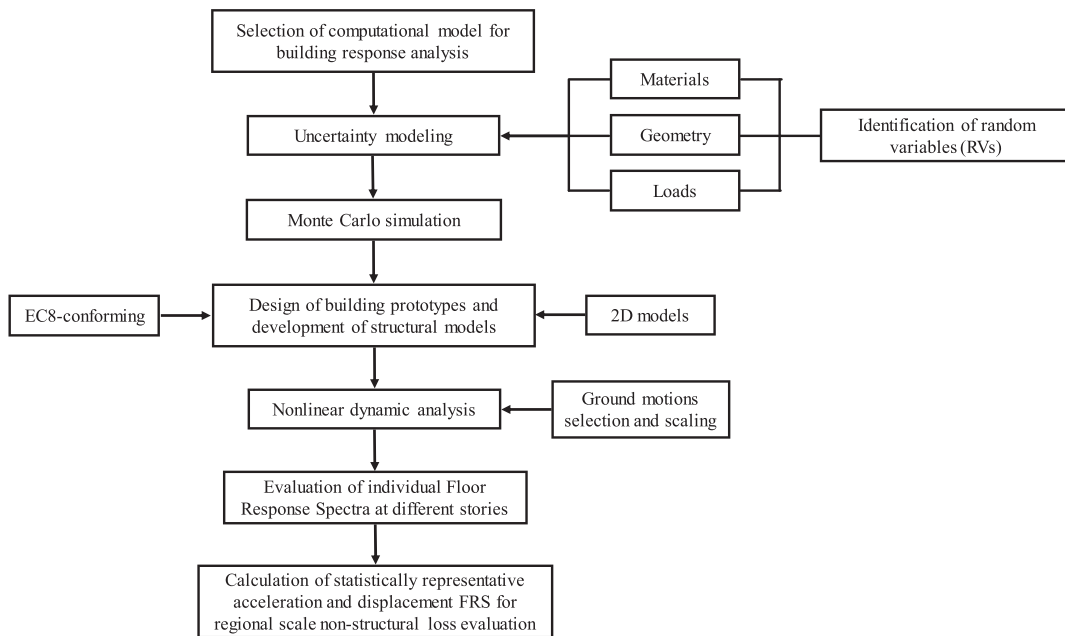


Fig. 1. Flowchart of the probabilistic floor response spectra evaluation.

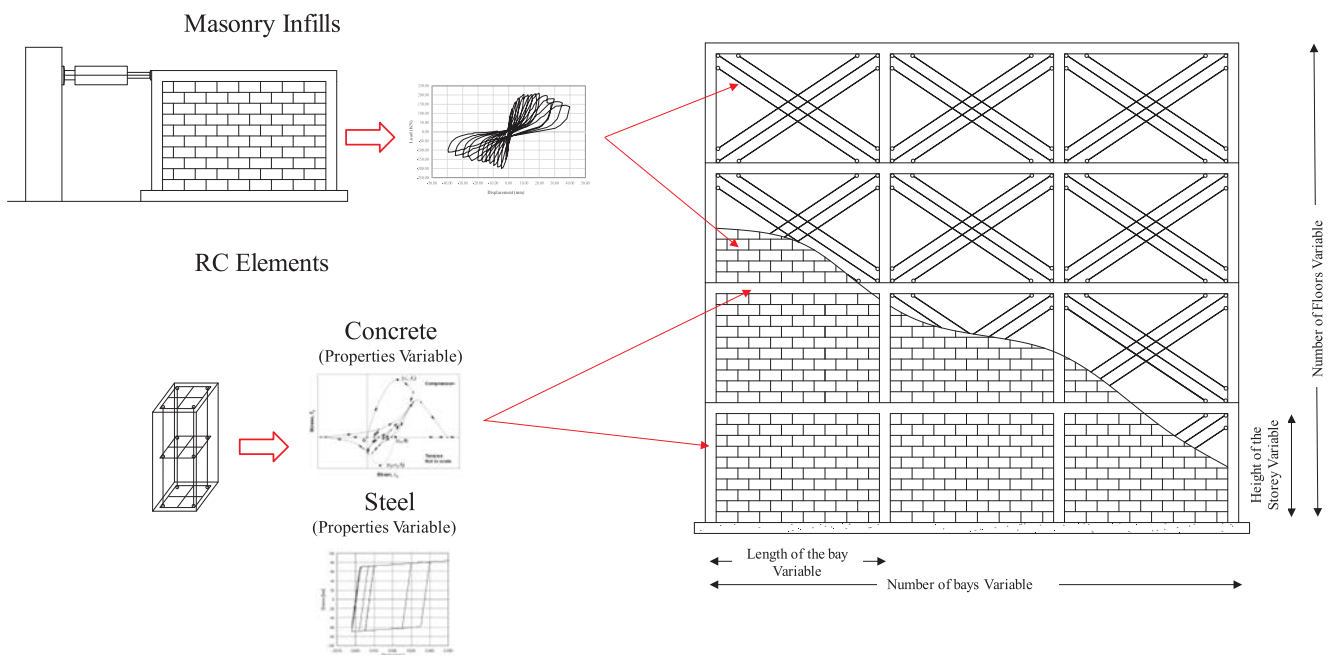


Fig. 2. Illustration of modelling parameters for RC case study buildings.

developed to carry out NLTHA and to evaluate the FRS at each floor level of interest (Fig. 2). The models were developed using the open source software OpenSees [41]. Except for the masonry infills, the interaction between the structural and other non-structural elements was neglected. According to this assumption, it is supposed that the non-structural elements do not affect the dynamic behaviour of the structures both in terms of stiffness and strength. The OOP behaviour of the unreinforced masonry infills as well as the influence of openings and irregular distribution of the masonry infills were not considered in the numerical modelling. The numerical models were developed assuming the fiber force-based approach [42]. Inelastic beam-column fiber elements were used to model the frame members, explicitly including geometric and material nonlinearities. A distributed plasticity approach was thus adopted to simulate the spreading of inelasticity over the

member length and cross section. The uniaxial confinement model proposed by Chang and Mander [43] was considered to simulate the cyclic behavior of concrete, the hysteretic rules of which were established based on statistical regression analysis on the experimental data from cyclic compression tests conducted by a number of researchers [43]. A simple bilinear constitutive model with isotropic strain hardening was assigned to the steel rebars.

Several approaches are available in the literature to consider the effects of masonry infills on the linear and nonlinear response of RC buildings. In this study, each masonry infill wall panel was modelled by an equivalent triple-truss model. The global stiffness of the panel was distributed among three parallel diagonal truss elements by assigning a rate of stiffness and strength equal to 50% to the central truss and equal to 25% to each of the off-diagonal trusses. The width of the struts ( $b_w$ ) is

based on the relationship proposed by Mainstone [44]:

$$\frac{b_w}{d} = 0.175\lambda_h^{-0.4} \quad (1)$$

where  $d$  is the diagonal length of the infill panels and  $\lambda_h$  is the relative panel-to-frame stiffness ratio introduced by Smith [45]. The relative panel-to-frame stiffness ratio,  $\lambda_h$ , is given by:

$$\lambda_h = \left( \frac{E_w t_w \sin(2\theta)}{4E_c I_p h_w} \right)^{0.25} \quad (2)$$

where  $E_w$  is the Young modulus of the masonry infills,  $t_w$  is the thickness of the panel,  $h_w$  is the height of the panel,  $E_c$  is Young's modulus of the concrete in the RC frame,  $I_p$  is the mean moment of inertia of the two RC columns confining the infill wall, and  $\theta$  is the slope angle of the panel's diagonal. All the parameters in Eq. (2) can be easily evaluated for a given floor of a building at the design stage. The results of the cyclic tests carried out by Cavaleri and Di Trapani [28] on clay masonry infill panels were used to calibrate the infill model using the Pinching4 material available in Opensees [42]. The effects of openings and non-uniform distribution of infill walls were not considered in this study. The beams' and columns' shear failure mechanism was not explicitly modelled, however a post-process analysis of the results was performed in order to verify this failure mechanism (which is not expected due to the design approach and the considered low seismic intensity). Rayleigh tangent stiffness proportional viscous damping was introduced in the numerical model with 5% of critical damping specified in the first two elastic modes of vibration. Note that the hysteretic damping has been explicitly modelled in the hysteretic behavior of the structural elements and of the infill panels. Newton-Raphson convergence criteria were implemented to iteratively equilibrate the loads.

### 3.3. Earthquake ground motions

A set of 20 horizontal accelerograms representative of frequent earthquake ground motions at the site of the case-study buildings were selected from the PEER NGA-West database [46]. Based on a preliminary estimation of the Italian and European seismicity, the selection of the site was carried out in order to represent a medium-to-high seismicity in Italy. In 2011, Stucchi *et al.* [47] performed a probabilistic seismic hazard assessment of Italy. Based on the results of this assessment, the Italian Building Code [48] provides a detailed hazard map characterized by a grid with more than 16,000 points corresponding to different probabilities of exceedance in 50 years of peak ground accelerations. A site close to the city of Cassino, in Italy, was chosen for the ground motion selection. This site is close to the areas struck by recent earthquakes in Italy (e.g. 2009 L'Aquila Earthquake and 2016 Central Italy Earthquake). This site is characterized by a peak ground acceleration on stiff soil equal to 0.21 g for a 10% probability of exceedance in 50 years (or 475 years return period). Because the Eurocode 8 does not provide a formulation to define the target spectrum for frequent (serviceability level) ground motions [12], the recommendations provided by the Italian Building Code were applied to define the target spectrum and to proceed with the ground motions selection. According to the Italian Building Code, a frequent earthquake is characterized by a 63% probability of exceedance in 50 years; this corresponds to a return period of 70 years. Hazard-consistent record selection was based on spectral compatibility (matching of the geometric mean) with a conditional mean spectrum according to the methodology proposed by Jayaram *et al.* [49]. This approach considers the conditional variance given a return period of spectral acceleration at the vibration periods of interest selected (0.2, 0.5 and 1.0 s). The conditional periods,  $T^*$ , to be used for the NLTHAs of individual building archetypes were selected based on the results of eigenvalue analyses, as discussed in the next section. Fig. 3 shows the mean response spectra and all individual record response spectra for the 20 considered ground motions for

$T^* = 0.2, 0.5$  and  $1.0$  s.

Seismic hazard calculations and derivation of the conditional mean spectra were performed with the REASSESS software [50], using the correlation model among spectral acceleration ordinates suggested by Baker and Jayaram [51]. The selected records were scaled up to a maximum scale factor of 3.0 to achieve spectral matching. Tables 1–3 list the main characteristics of the final scaled ground motions for conditional periods  $T^* = 0.2, 0.5$  and  $1.0$  s, respectively.

## 4. Analysis results

In this section, the results of the NLTHs on the masonry infilled RC frame archetypes are presented in terms of elastic periods, absolute acceleration FRS, and relative displacement FRS. The RC frame archetypes are grouped by number of floors and the results are presented across all other RVs in order to evaluate trends. It is worth noting that, due to the low seismic intensity, both structural elements and masonry infills do not necessarily experience nonlinear behavior, although the numerical modelling framework proposed in this study takes explicitly into account nonlinearities both in the structure and in the infills, something which renders the adopted/proposed modelling framework more general and applicable to higher intensities. This consideration could lead to a simplification of the numerical models if only the elastic seismic response of the structures, for low seismic intensity, need to be investigated.

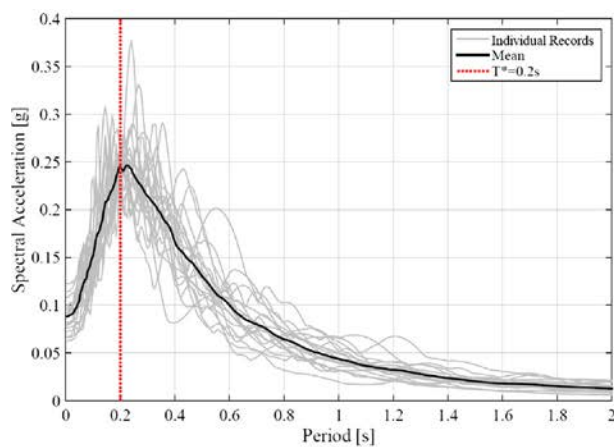
### 4.1. Elastic period

Fig. 4 shows the computed elastic fundamental periods for all 100 building archetypes without (Fig. 4a) and with (Fig. 4b) masonry infills as a function of building height. These results lay evident that the masonry infills, acting as equivalent diagonal struts, increase the stiffness of the primary structures. Two main observations can be made from the results:

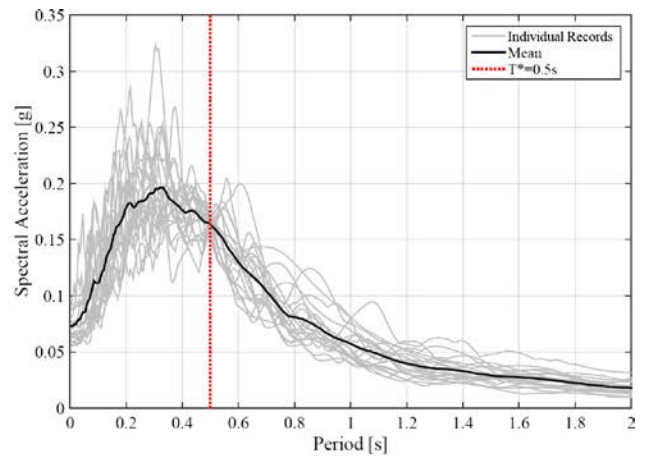
1. As expected, the fundamental periods are significantly shortened when masonry infills are introduced. For the studied building population, the percentage in the reduction of fundamental period due to the presence of the infills ranges between 19% and 49%.
2. The variations in fundamental periods with building height are reduced by the presence of the masonry infills, as demonstrated by the lower dispersion of the computed periods for frames of a given height. The difference between the maximum and minimum periods for the bare six-story frames is equal to 38%, while it reduces to 25% when the infilled walls are included.

As discussed by Perrone *et al.* [23], a fundamental parameter governing the influence that masonry infills have on the elastic period of a reinforced concrete frame is the relative panel-to-frame stiffness ratio,  $\lambda_h$  (see Eq. (2)). It quantifies the differences in stiffness between the RC columns and the masonry panels in a story. The high variability in the periods of the bare frames, in particular for middle-rise frames (frames with 3, 4, and 6 storeys), is mainly related to the variation in the number and length of the bays. For the six-story bare frames, for example, the mean value of the period equals to 0.91 s and 0.75 s, respectively for frames with 3 and 6 bays. The eigenvalue results also showed that the material properties, as well as the inter-story height, have a minor influence on the period estimate. The variability in the fundamental period is reduced by the presence of masonry infills due to their significant contribution to the story stiffness. In particular, focusing on the six-story infilled frames, the mean fundamental period is equal to 0.58 s and 0.54 s, for frames with 3 and 6 bays, respectively.

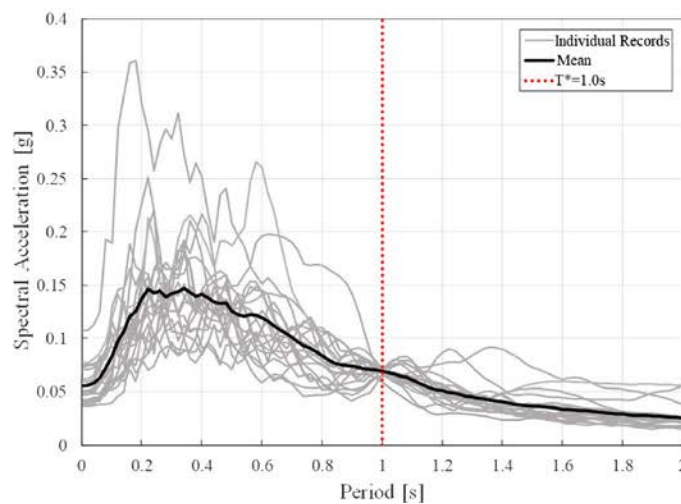
Some simplified equations have been developed to evaluate the elastic fundamental period,  $T$ , of masonry infilled RC frames (e.g. [22,23]). The equations are expressed in the following form:



a) Conditional period  $T^* = 0.2$  s.



b) Conditional period  $T^* = 0.5$  s.



c) Conditional period  $T^* = 1.0$  s.

Fig. 3. Mean response spectrum and acceleration response spectra of all considered ground motions for a conditional period,  $T^*$ , equals to (a) 0.2 s, (b) 0.5 s and (c) 1.0 s.

Table 1

Main characteristics of scaled ground motions for conditional period  $T^* = 0.2$  s.

Earthquake ID	Earthquake name	Date	Moment magnitude	Epicentral distance (km)	PGA (g)	Scale factor
0078	Coalinga/03	06/11/1983	5.38	15.56	0.17	0.43
3210	Chi/Chi, Taiwan/05	09/22/1999	6.20	71.18	0.13	0.56
2169	Chi/Chi, Taiwan/02	09/20/1999	5.90	65.55	0.09	0.99
205	Imperial Valley/07	10/15/1979	5.01	9.08	0.16	0.52
714	Whittier Narrows/02	10/04/1987	5.27	7.33	0.30	0.26
627	Whittier Narrows/01	10/01/1987	5.99	26.21	0.15	0.42
412	Coalinga/05	07/22/1983	5.77	16.17	0.43	0.19
658	Whittier Narrows/01	10/01/1987	5.99	66.43	0.04	1.68
2995	Chi/Chi, Taiwan/05	09/22/1999	6.20	49.79	0.03	0.78
385	Coalinga/02	05/09/1983	5.09	8.09	0.16	0.44
998	Northridge/01	01/17/1994	6.69	27.29	0.37	0.18
540	N.Palm Springs	07/08/1986	6.06	4.24	0.60	0.14
5	Northwest Calif/01	06/10/1938	5.50	54.88	0.11	0.69
1076	Northridge/01	01/17/1994	6.69	51.96	0.14	0.46
486	Taiwan SMART1(33)	06/12/1985	5.80	44.93	0.06	1.07
1738	Northridge/06	03/20/1994	5.28	9.02	0.25	0.36
140	Tabas, Iran	09/16/1978	7.35	117.66	0.11	0.91
44	Lytle Creek	09/12/1970	5.33	31.48	0.04	1.99
102	Northern Calif/07	06/07/1975	5.20	10.42	0.11	0.46
422	Trinidad offshore	08/24/1983	5.70	71.24	0.13	0.65

**Table 2**  
Main characteristics of scaled ground motions for conditional period  $T^* = 0.5$  s.

Earthquake ID	Earthquake Name	Date	Moment magnitude	Epicentral distance (km)	PGA (g)	Scale factor
3005	Chi/Chi, Taiwan/05	09/22/1999	6.20	51.79	0.04	1.68
1093	Northridge/01	01/17/1994	6.69	80.25	0.04	1.27
223	Livermore/02	01/27/1980	5.42	16.57	0.19	0.33
2160	Chi/Chi, Taiwan/02	09/20/1999	5.90	53.57	0.05	0.99
972	Northridge/01	01/17/1994	6.69	86.45	0.10	0.62
189	Imperial Valley/06	10/15/1979	6.53	12.43	0.36	0.16
616	Whittier Narrows/01	10/01/1987	5.99	7.50	0.19	0.29
602	Whittier Narrows/01	10/01/1987	5.99	26.55	0.19	0.33
1001	Northridge/01	01/17/1994	6.69	33.77	0.27	0.23
711	Whittier Narrows/02	10/04/1987	5.27	20.52	0.16	0.54
306	Taiwan SMART1(5)	01/29/1981	5.90	30.31	0.11	0.58
984	Northridge/01	01/17/1994	6.69	41.01	0.17	0.42
2162	Chi/Chi, Taiwan/02	09/20/1999	5.90	80.45	0.03	2.96
1259	Chi/Chi, Taiwan	09/20/1999	7.62	63.93	0.09	0.62
955	Northridge/01	01/17/1994	6.69	68.68	0.11	0.55
936	Big Bear/01	06/28/1992	6.46	156.97	0.03	1.81
3452	Chi/Chi, Taiwan/06	09/25/1999	6.30	78.85	0.05	1.01
224	Livermore/02	01/27/1980	5.42	21.65	0.05	1.06
591	Whittier Narrows/01	10/01/1987	5.99	28.50	0.06	1.19
1087	Northridge/01	01/17/1994	6.69	5.41	1.66	0.05

**Table 3**  
Main characteristics of scaled ground motions for conditional period  $T^* = 1.0$  s.

Earthquake ID	Earthquake name	Date	Moment magnitude	Epicentral distance (km)	PGA (g)	Scale factor
996	Northridge/01	01/17/1994	6.69	16.99	0.25	0.62
1082	Northridge/02	01/17/1995	6.69	12.35	0.36	0.38
1297	Chi-Chi, Taiwan	09/20/1999	7.62	74.12	0.15	1.42
944	Northridge/01	01/17/1994	6.69	70.45	0.07	1.94
799	Loma Prieta	10/18/1989	6.93	79.13	0.28	0.55
165	Imperial Valley-06	10/15/1979	6.53	18.88	0.27	0.90
2378	Chi-Chi, Taiwan-02	09/20/1999	5.90	58.25	0.07	1.62
949	Northridge-01	01/17/1994	6.69	11.10	0.33	1.84
27	Hollister-02	04/09/1961	5.50	18.92	0.07	2.90
3328	Chi-Chi, Taiwan-06	09/25/1999	6.30	60.22	0.04	1.43
12	Kern Country	07/21/1952	7.36	118.26	0.05	1.49
2410	Chi-Chi, Taiwan-02	09/20/1999	5.90	44.86	0.50	0.15
322	Coalinga-01	05/02/1983	6.36	30.06	0.28	0.27
367	Coalinga-01	05/02/1983	6.36	9.98	0.32	2.93
312	Taiwan SMART1(5)	01/29/1981	5.90	28.67	0.08	0.11
1806	Hector Mine	10/16/1999	7.13	185.09	0.05	0.70
778	Loma Prieta	10/18/1989	6.93	45.10	0.26	1.02
576	Taiwan SMART1(45)	11/14/1986	7.30	75.25	0.16	2.29
1776	Hector Mine	10/16/1999	7.13	74.27	0.07	0.87
1276	Chi-Chi, Taiwan	09/20/1999	7.62	81.66	0.11	1.03

$$T = \alpha H^\beta \tag{3}$$

where H is the height of the building expressed in meters. Ricci *et al.* [22] proposed a linear relationship in order to evaluate the fundamental period of infilled frames, assuming  $\alpha = 0.031$  and  $\beta = 1.0$  in Eq. (3). This empirical equation approximates very well the results obtained herein. In particular from a linear regression analysis on the

eigenvalue results yields that the best-fit parameters of Eq. (3) are  $\alpha = 0.032$  and  $\beta = 1.0$ , as shown in Fig. 4b. A similar equation, in which the parameter  $\alpha$  is a function of Young's Modulus of the masonry panels was also proposed by Perrone *et al.* [23]. Based the Young's modulus of the masonry considered for the building population, the value of  $\alpha$  to be used in Eq. (3) is equal to 0.033. Perrone *et al.* [23] also

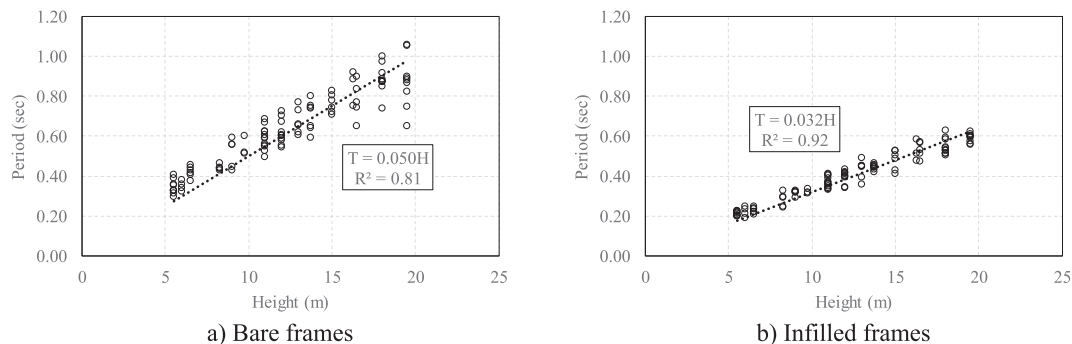


**Fig. 4.** Elastic period of the RC moment resisting frame population.

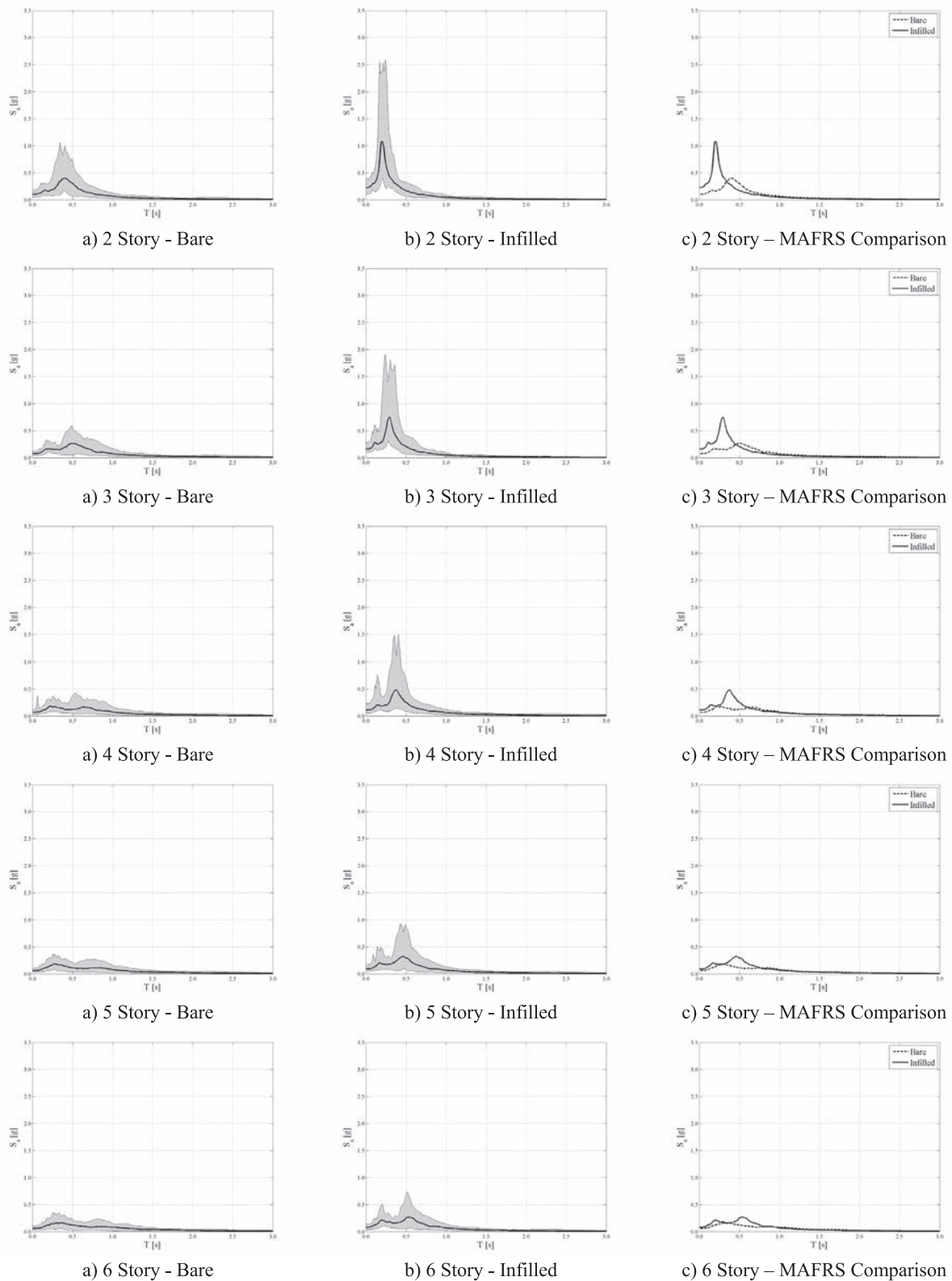


Fig. 5. Comparison of first floor acceleration response spectra.

proposed an equation for RC bare frames in which  $\alpha = 0.052$  and  $\beta = 1.0$ ; this equation is again very close to the results of the regression analysis performed for the present study, in which  $\alpha = 0.50$  and  $\beta = 1.0$ , as shown in Fig. 4a.

#### 4.2. Absolute acceleration floor response spectra

In this section, the results of the NLTHAs are presented in terms of absolute acceleration floor response spectra (AFRS). The 5% damped AFRS were evaluated by subjecting the building archetypes to the selected set of ground motions and then using numerical techniques to

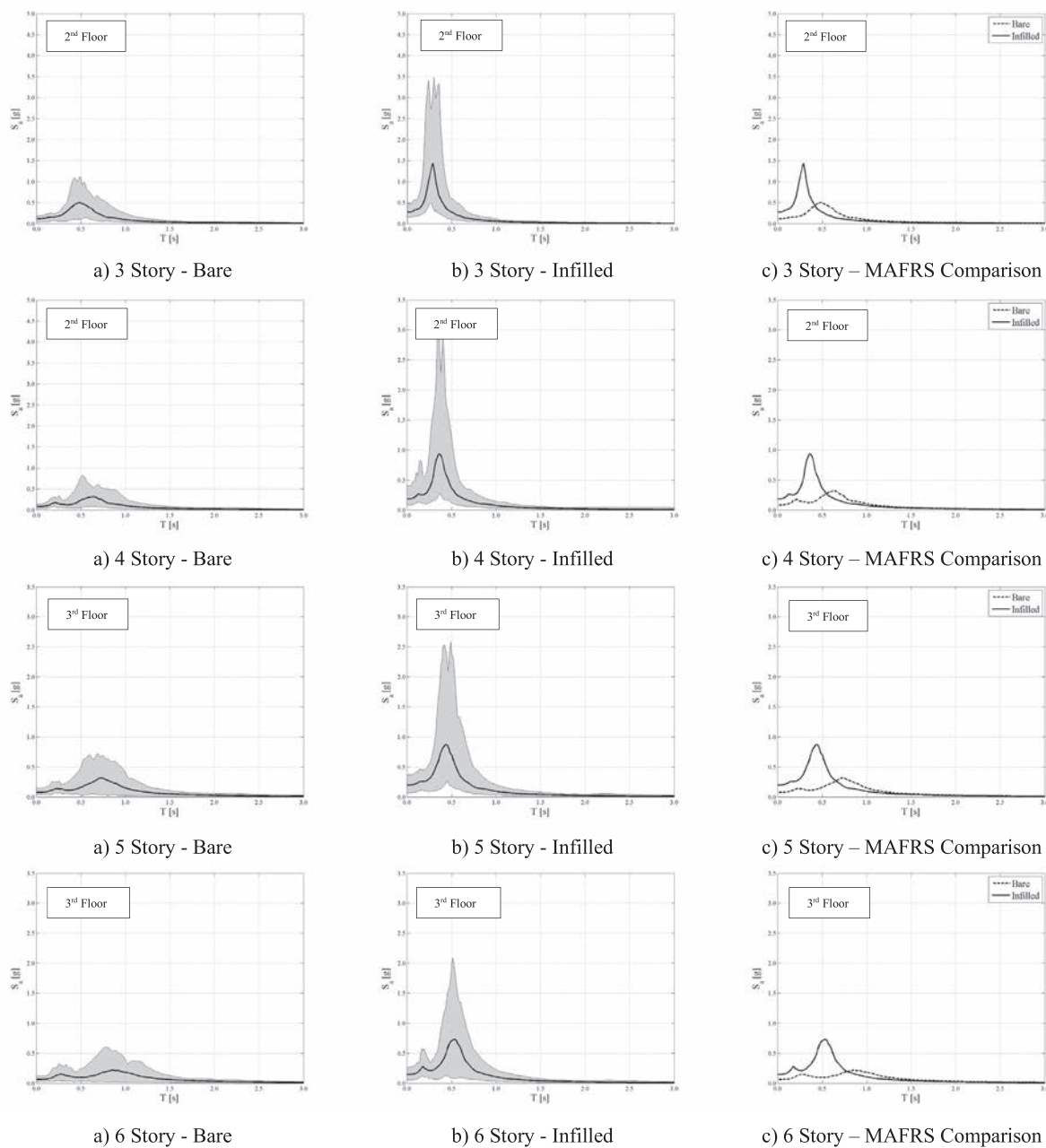


Fig. 6. Comparison of acceleration mid-height floor response spectra.

compute the FRS from floor acceleration time-histories recorded along the structure's height. The median acceleration floor response spectra (MAFRS) taken across the ground motions ensemble were evaluated – for each story of each RC frame – with and without considering masonry infills. The 5% damped MAFRS spectra obtained for the bare and in-filled frames are plotted and compared in Figs. 5–7. In each plot, the MAFRS for both bare (Figs. 5a, 6a and 7a) and in-filled (Figs. 5b, 6b and 7b) frames are shown for three representative floors of the frames (i.e. first, mid-height and top floor). The solid lines in Figs. 5–7 represents the MAFRS across all the RC frames characterized by the same number of stories, while the grey-filled area represents the envelope of all individual building archetype AFRS. The filled area is representative of the record-to-record variability as well as of the variability due to the RVs considered (i.e. number and length of the bays, live loads and material properties). Evaluation of the variability in MAFRS is paramount for regional scale seismic loss estimation, in which the high variability in the building portfolio could significantly affect the results.

The MAFRS for a given single RC frame, in which only the record-to-record variability is taken into account, starts from a spectral acceleration at zero period equals to the median peak floor acceleration and then it is generally characterized by a single peak spectral acceleration that lies at the fundamental period of the structure, if the structure behaves elastically. After the peak the spectral acceleration, the MAFRS reduces to zero for very long periods. Contrarily, the peak spectral accelerations of MAFRS reported in Figs. 5–7 are representative of a set of RC frames characterized by the same number of floors but with different geometrical and mechanical properties; consequently, the peak spectral accelerations are representative of a wider range of periods. This behaviour is particularly pronounced for the taller bare frames (Figs. 5a–7a). This increased variability in predominant floor spectra periods for taller frames can be also seen in Fig. 4a. For the bare RC frames, the influence of the higher modes is evident in many cases, with the highest influence being observed, again, in taller frames. The contribution of higher modes is more evident in the lower floors, in which

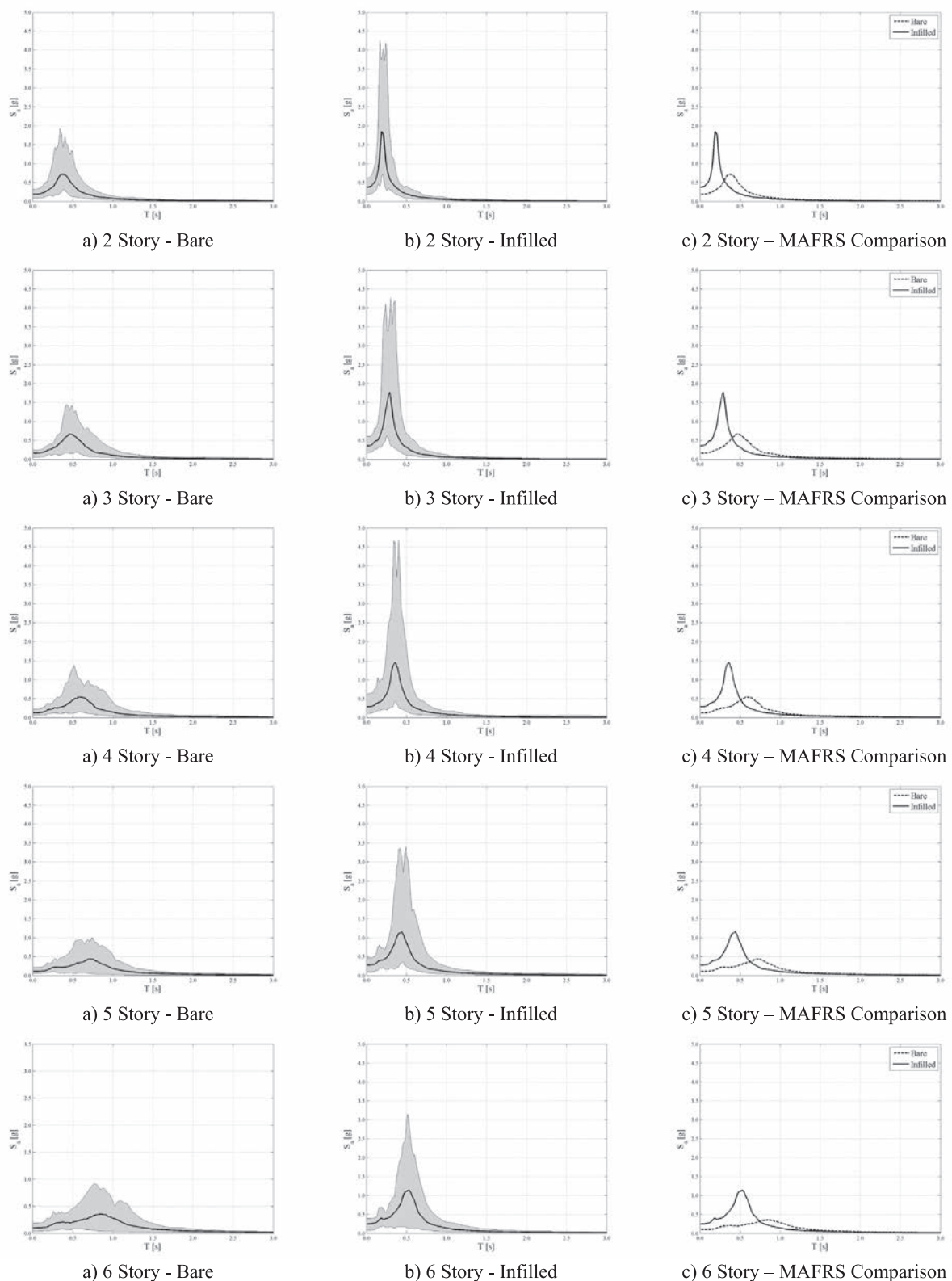


Fig. 7. Comparison of top floor acceleration response spectra.

the median peak spectral accelerations for short periods are comparable to those at longer periods (e.g. Fig. 5a).

In the masonry infilled RC frames, the variation of the fundamental periods due to the variability in the geometrical and mechanical properties is lower, and this behavior can be seen from the MAFRS (Figs. 5b–7b). The MAFRS for the masonry infilled RC frames are

generally characterized by a well-defined single peak that lies at a period close to the fundamental period of the structure with steep drops off for other periods. This behavior can be associated to the stiffness and strength increase caused by the explicit modeling of the infilled walls in these frames.

Comparing the MAFRS for the bare and infilled frames Figs. 5c, 6c

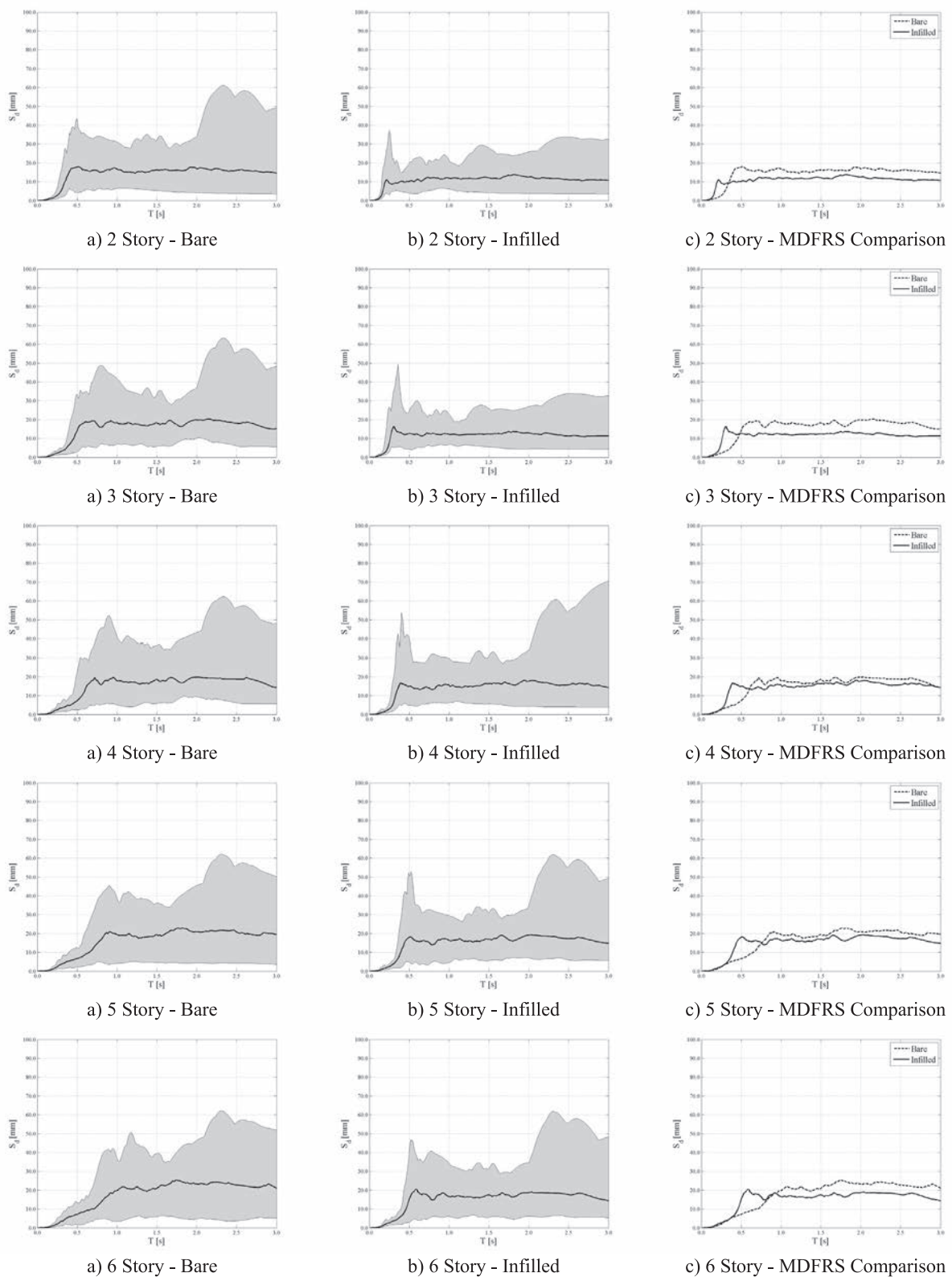


Fig. 8. Comparison of first floor relative displacement response spectra.

and 7c, two main effects can be observed: (1) the spectral peaks are shifted to shorter periods corresponding to the natural periods of the buildings with masonry infills, and (2) the amplitudes of the spectral peaks are significantly increased. For example, the median peak spectral acceleration of the in-filled RC frames at the top floor increases by 114% and 140%, for the 2-story and 6-story RC frames, respectively.

These two effects can be observed for all floors in all frames. The higher floor spectral accelerations in the in-filled RC frames are related both to the higher ground spectral accelerations in the range of periods of the in-filled RC frames and to changes in their dynamic properties. The higher participating mass associated to the first mode and the different mode shapes also contributed to increase the floor spectral

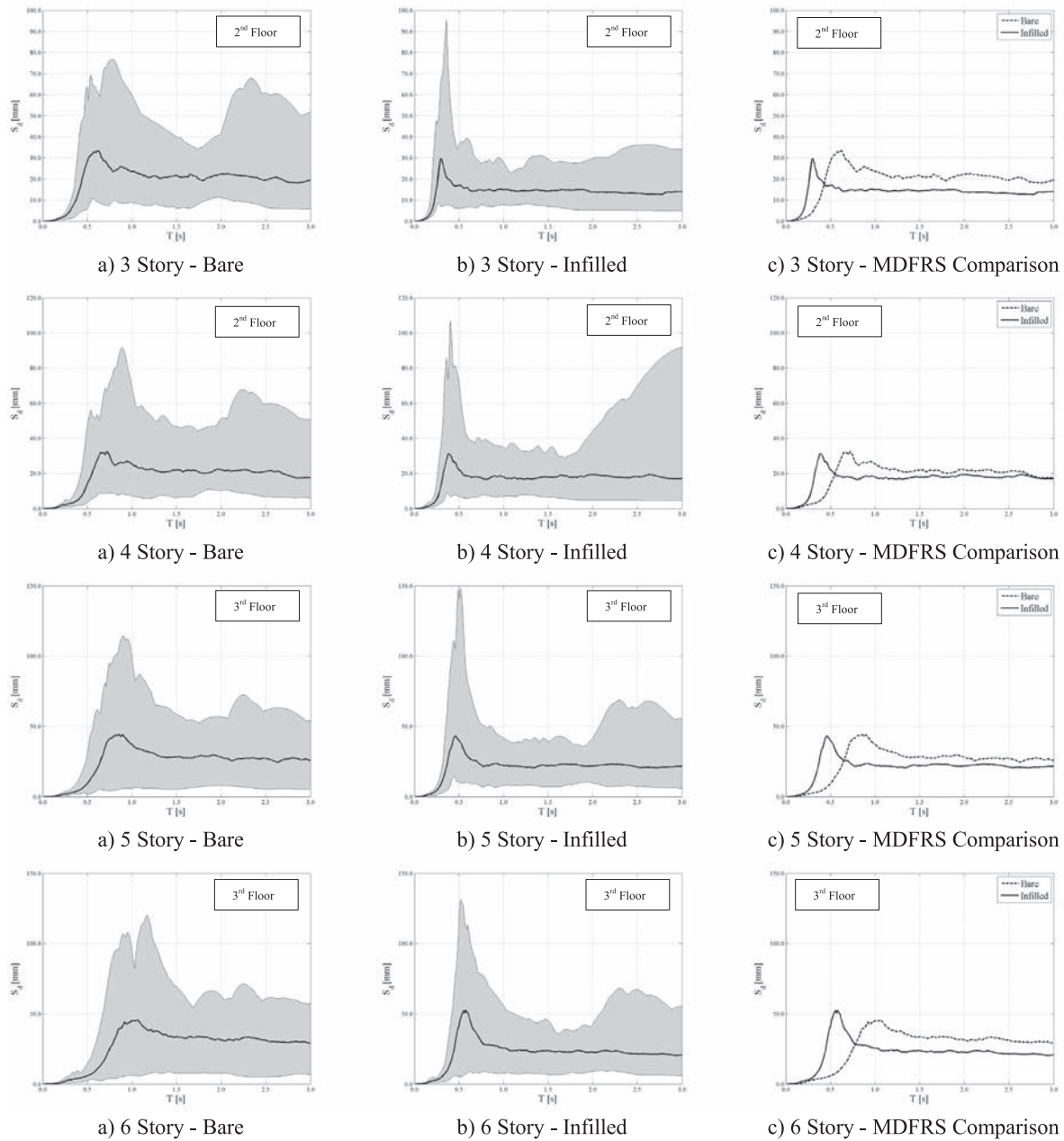


Fig. 9. Comparison of mid-height relative displacement floor response spectra.

accelerations with respect to the bare frames. The shape of the MAFRS is also significantly influenced by the presence of masonry infills. For the infilled frames, a higher dispersion is observed close to the fundamental periods of the frames, while the dispersion significantly decreases for the other periods; this is mainly due to the steep drops in spectral accelerations away from the fundamental periods. For the bare frames, on the other hand, higher dispersions of the spectral accelerations occur even for periods far from the fundamental periods.

#### 4.3. Relative displacement floor response spectra

In this section, the results of the NLTHAs are presented in terms of relative displacement floor response spectra (DFRS). Similar to the AFRS of Section 4.2, the DFRS envelopes and median DFRS (MDFRS) are shown for the lower, mid-height and top floors of the building population (Figs. 8–10). Again here, the DFRS of all RC frames characterized by the same number of floors are plotted together in order to

quantify the influence of uncertainties in the geometry, material properties and design loads as well as to characterize the record-to-record variability.

The general shape of a DFRS starts at zero period with a spectral displacement equal to zero, then the spectral displacement increases and reaches the maximum value at the fundamental period of the frame. After the peak, the spectral displacement reduces and tends to the maximum absolute displacement of the floor for very long periods. This shape of the DFRS is generally observed at the upper floors of the frames, while a more irregular spectral shape is often observed at the lower floors. Comparing the MDRFS for both bare and infilled frames, two pivotal effects associated with the explicit modeling of the masonry infills can be singled out: (1) for the infilled frames, the peak spectral displacements are shifted to shorter periods, and (2) the median peak spectral displacements in bare and infilled configurations are of similar amplitudes with no particular trend. The peak spectral displacements for short infilled frames are smaller than that of short bare frames,

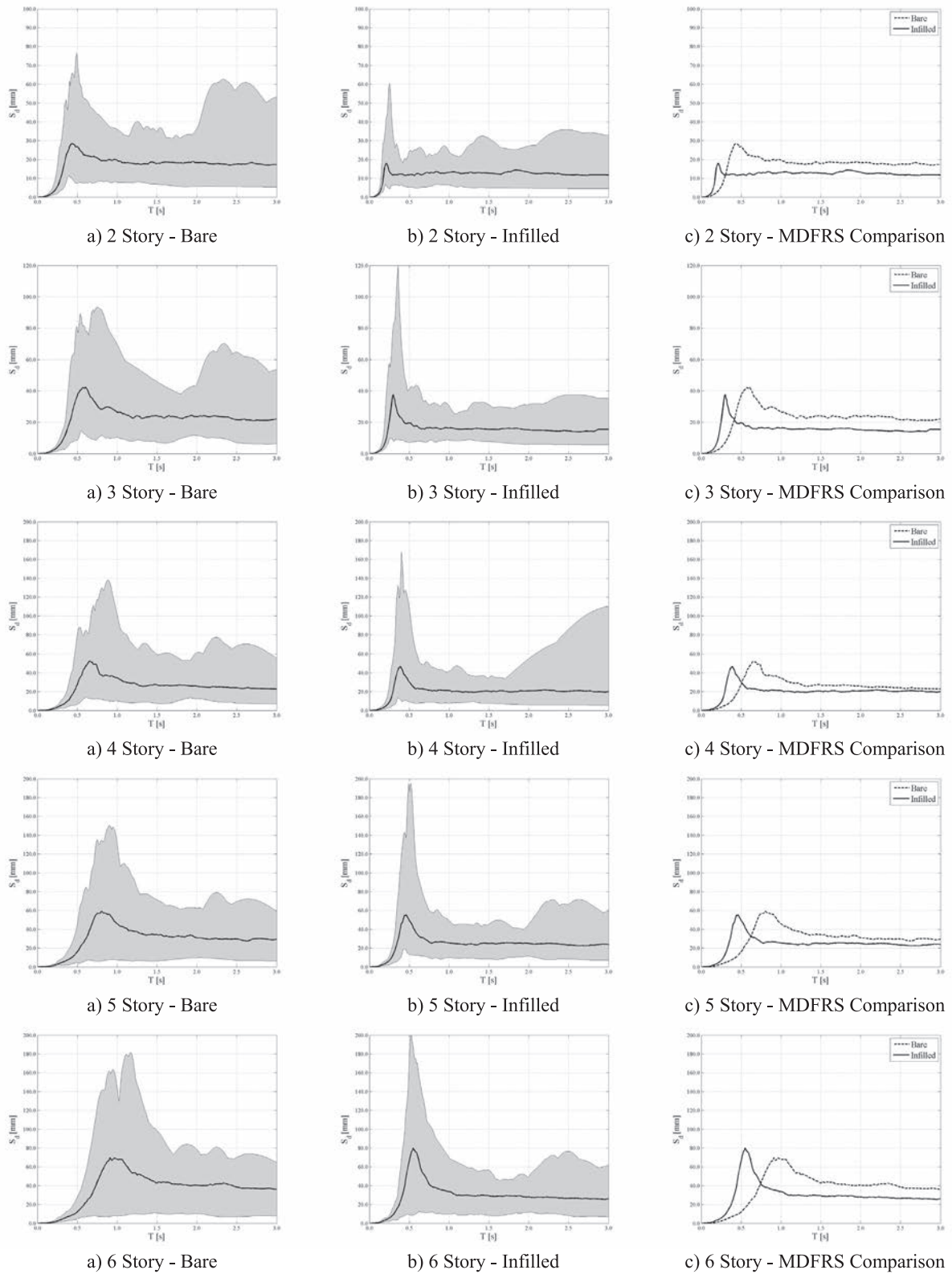


Fig. 10. Comparison of top floor relative displacement response spectra.

while they are comparable for taller frames. This trend, opposite to that observed for the AFRS, is the result of the higher stiffness of the infilled frames. This differences in spectral displacement amplitudes can be explained by computing the ratios between the spectral displacements of the bare ( $S_{DF,b}$ ) and infilled ( $S_{DF,i}$ ) frames using the usual pseudo-spectra formula [52]:

$$S_{DF} = \frac{T^2}{4\pi^2} S_{AF} \tag{4}$$

$$\frac{S_{DF,b}}{S_{DF,i}} = \frac{S_{AF,b}}{S_{AF,i}} \cdot \left(\frac{T_b}{T_i}\right)^2 \tag{5}$$

**Table 4**  
Ratios between top floor median peak  $S_{DF,b}$  and  $S_{DF,i}$ .

	2 Storey	3 Storey	4 Storey	5 Storey	6 Storey
MDFRS	1.56	1.12	1.11	1.06	0.87
Eq. (5)	1.56	1.14	1.10	1.08	0.85

Table 4 compares the median peak ratios  $S_{DF,b}/S_{DF,i}$  at the top floors of the RC frame archetypes obtained from the MDFRS and by Eq. (5). The ratios and trend observed in the MDFRS are well predicted by Eq. (5). Clearly, the main parameter governing the  $S_{DF,b}/S_{DF,i}$  ratios are the square of the structural period ratios ( $T_b/T_i$ ).

The envelopes of all the DFRS plotted in Figs. 8–10 indicate higher dispersions in spectral displacement amplitudes as a result of the RVs taken into account in the design of the frames, as well as of the record-to-record variability. This can also be shown by analysing the periods at which the spectral displacement peaks lie; for the bare frames, the period range is wider than for the infilled configurations.

## 5. Implications of results on regional scale seismic loss estimation

In a regional risk model, the buildings' response is generally assessed using the capacity spectrum method by intersecting the acceleration-displacement demand spectrum with the building capacity curve. Damage state probabilities are converted into monetary losses using inventory information and economic data. For a given building typology, the intersection between the capacity curve and the demand spectrum, the demand in terms of spectral displacement is obtained. The recorded spectral displacements are thus used to define, for structural components and displacement-sensitive non-structural elements, the cumulative probability of being in, or exceeding, a particular damage state.

According to the widely used HAZUS methodology [11] for regional scale loss estimation studies, two sub-categories of acceleration-sensitive non-structural elements are considered: elements at or near the ground level and elements at the upper floors of buildings. For both sub-categories, the fragility functions are defined in terms of peak floor acceleration. However, in order to simplify the calculations, the peak ground acceleration is assumed to be more representative of the seismic demand on non-structural elements located at the near ground levels, while the ground spectral acceleration at the fundamental period of the building is assumed to define the seismic demand for acceleration-sensitive non-structural elements located at the upper floors. The HAZUS methodology assumed that 50% (for low-rise), 33% (for mid-rise) and 20% (for high-rise) of non-structural elements are located at, or near, the ground floor, while 50% (for low-rise), 66% (for mid-rise) and 80% (for high-rise) of non-structural elements are located at the upper floors.

Using the results obtained above, Fig. 11 compares the median acceleration ground response spectra with the median absolute acceleration floor response spectra (MAFRS) at the first (Fig. 11a) and at the top level (Fig. 11b) for both bare and infilled frame archetypes. The MAFRS include the entire building population considered in this study. Although the median ground response spectrum and the MAFRS are plotted together, the period at which the response spectra refer to are different. The median ground response spectrum refers to the period of the supporting structure while the MAFRS refer to the period of the non-structural elements ( $T_{NSE}$ ). In order to improve the HAZUS methodology based on the results obtained in this study, two different approaches can be used. In the first approach, the acceleration sensitive non-structural elements are considered rigid (this approach is consistent with the HAZUS methodology), while in the second approach the non-structural elements are considered flexible (assuming known values of  $T_{NSE}$ ).

For non-structural elements located at the first floor of buildings, the HAZUS methodology takes the seismic demand equal to the PGA (0.05 g in Fig. 11). Table 5 lists the spectral accelerations at which the non-structural elements are subjected, for different values of  $T_{NSE}$ . The percentage increases with respect to the HAZUS methodology are indicated in brackets. As reported in Table 5, the seismic demand on the non-structural elements is significantly underestimated both if the non-structural elements are assumed rigid or flexible. The difference increases significantly when the influence of the masonry infills is considered.

For non-structural elements located at the top floor of buildings, the HAZUS methodology takes the ground spectral acceleration at the median periods for the entire building population considered in this study ( $T = 0.62$  s and  $T = 0.41$  s for bare and infilled frames, respectively) as seismic demand. Table 6 lists the spectral accelerations at which the non-structural elements are subjected for different values of  $T_{NSE}$ . Again, the percentage difference increases with respect to the HAZUS methodology is indicated in bracket. Again for non-structural elements located at the upper floors, the seismic demand is significantly underestimated by the HAZUS methodology.

A comparison between the HAZUS methodology and the obtained results, in terms of seismic demand for displacement-sensitive non-structural elements, is not carried out herein because, according to the HAZUS methodology, the pushover curves for all the RC frames of the database are required; something which is out of the scope of this research.

Clearly, a more refined evaluation of damage and losses in acceleration-sensitive non-structural elements would require an improved engineering demand parameter. Many studies available in the literature (see e.g. [14–17]) demonstrated that the structural dynamic filtering significantly amplifies the accelerations from the ground to the upper floors of a building. Some simplified procedures were developed to

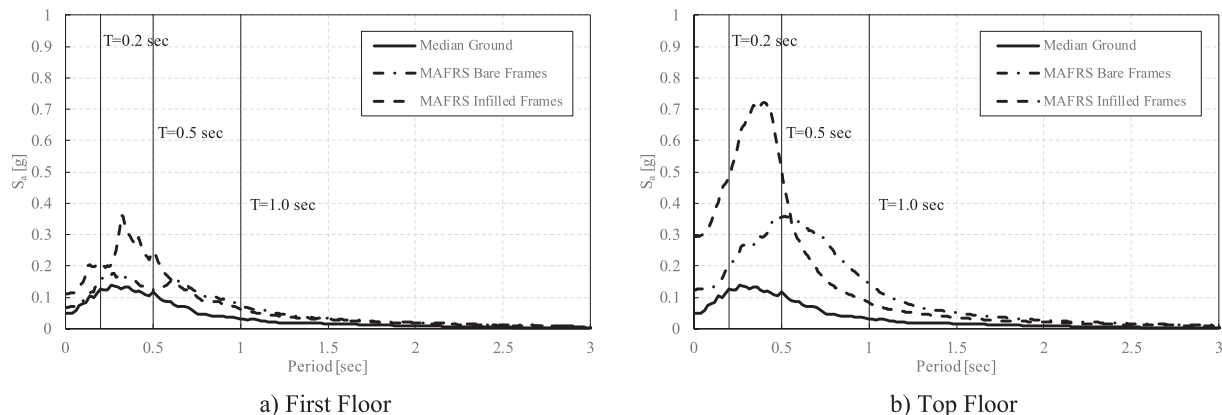


**Fig. 11.** Comparison between the median acceleration ground response spectrum and the median absolute acceleration floor response spectrum.

**Table 5**  
Comparison of the seismic demand for a non-structural element located at the first floor [g].

	HAZUS	$T_{NSE} = 0$ s	$T_{NSE} = 0.2$ s	$T_{NSE} = 0.5$ s	$T_{NSE} = 1.0$ s
Bare RC buildings	0.05	0.07 (40%)	0.16 (220%)	0.13 (160%)	0.08 (60%)
Infilled RC buildings	0.05	0.11 (120%)	0.21 (320%)	0.25 (400%)	0.07 (40%)

**Table 6**  
Comparison of the seismic demand for a non-structural element located at the top floor [g].

	HAZUS	$T_{NSE} = 0$ s	$T_{NSE} = 0.2$ s	$T_{NSE} = 0.5$ s	$T_{NSE} = 1.0$ s
Bare RC buildings	0.08	0.13 (63%)	0.20 (150%)	0.36 (350%)	0.14 (75%)
Infilled RC buildings	0.11	0.29 (164%)	0.48 (336%)	0.51 (364%)	0.09 (-18%)

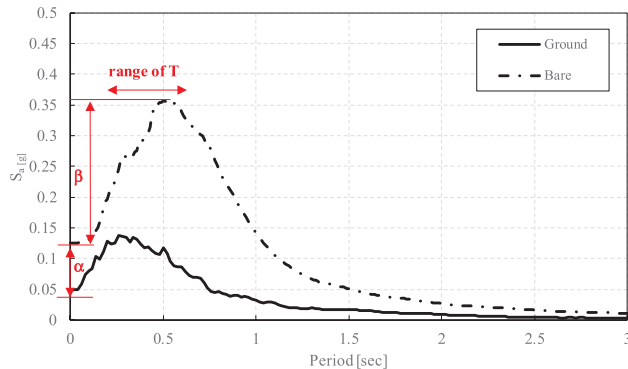


**Fig. 12.** Parameters required to calculate the median acceleration floor response spectrum.

**Table 7**  
Parameters required to evaluate the median top acceleration floor response spectrum for low-rise RC buildings.

	$\alpha$	$\beta$	Range of period (T)
Bare RC buildings	3.19	3.28	0.38–0.58 s
Infilled RC buildings	6.94	2.90	0.22–0.35 s

**Table 8**  
Parameters required to evaluate the median top acceleration floor response spectrum for medium-rise RC buildings.

	$\alpha$	$\beta$	Range of period (T)
Bare RC buildings	2.33	3.29	0.58–0.87 s
Infilled RC buildings	5.62	3.45	0.35–0.56 s

evaluate the floor response spectra starting from the ground spectrum and the modal properties of the buildings [14–17]. Although some of these methods are quite accurate for predicting the floor response spectra, two main issues arise: (1) all the methodologies were developed for bare frames without considering the influence of the masonry infills, and (2) these methodologies are generally not feasible for regional scale risk models because they require evaluation of the modal properties for each structure in the building portfolio.

There is a need to develop a simplified methodology to evaluate the seismic demand on acceleration-sensitive non-structural elements in regional risk models, taking into account masonry infills. In such simplified method, the following three parameters could be sufficient to predict the median floor response spectra without the need to perform structural analyses (see Fig. 12):

- 1) Spectral acceleration at zero period ( $T = 0$ ): the spectral acceleration at zero period can be obtained by multiplying the peak ground

spectral acceleration by an amplification factor,  $\alpha$ , for rigid non-structural elements;

- 2) Peak spectral acceleration (plateau): this value can be obtained by multiplying the spectral acceleration at zero period by an amplification parameter,  $\beta$ , that accounts for the non-structural amplification and for possible resonance phenomena; and
- 3) Period range of the plateau: contrary to the floor response spectrum for a single building, the median peak spectral acceleration does not lie at a single period value but is spread over a range of periods, which are representative of the building typology of interest. For this reason, a range of periods need to be identified to characterize the plateau of the median acceleration floor response spectrum.

Once these three parameters are defined, the median acceleration floor response spectrum can be simply estimated by constructing the following three branches: (1) a linear branch from  $T = 0$  to the lower period of the plateau,  $T_{low}$ ; (2) a constant branch from  $T_{low}$  to  $T_{high}$ ; (3) a decreasing branch proportional to  $1/T^2$  for periods longer than  $T_{high}$ .

Note that such an approach requires a new engineering demand parameter for non-structural elements (spectral acceleration at  $T_{NSE}$ ) and, therefore, recalibrated non-structural fragility functions. Conservatively, the ground response spectra could be amplified for all periods within the existing HAZUS methodology.

The feasibility of the improved non-structural demand evaluation proposed above was evaluated based on the results generated in this study. Tables 7 and 8 list the parameters  $\alpha$  and  $\beta$  required to predict the median acceleration floor response spectra for the bare and masonry infilled RC frame building population considered in this study. These  $\alpha$  and  $\beta$  parameters were calibrated according to the results of the NLTHAs. In regional scale studies, the building portfolios are generally divided into three categories: low-rise, medium-rise and high-rise buildings. For the purpose of comparison, the two and three-storey RC frames were assumed low-rise category buildings, while the four to six-storey RC frames were assumed to be medium-rise buildings. Figs. 13 and 14 compares the median top floor acceleration response spectra obtained from the NLTHAs for the bare (Figs. 13a and 14a) and infilled (Figs. 13b and 14b) RC frames, along with the acceleration floor response spectra predicted by the simplified methodology.

Good agreements can be observed between the predicted spectra and that generated from NLTHAs. The spectral accelerations are slightly overestimated in all cases. Note that the results presented are for a single ground motions return period of 70 years. Further analyses are required to fit/calibrate the model parameters for different ground motion return periods.

Similar results could be obtained using floor pseudo-acceleration spectra instead of floor absolute acceleration spectra. For periods and damping values of practical interest, these two quantifies are comparable and floor pseudo-acceleration spectra can be also used to derive floor relative displacement spectra. However, for the seismic design/assessment of most of NSEs the absolute acceleration at the centre of mass of the NSEs is usually used and for this reason the authors

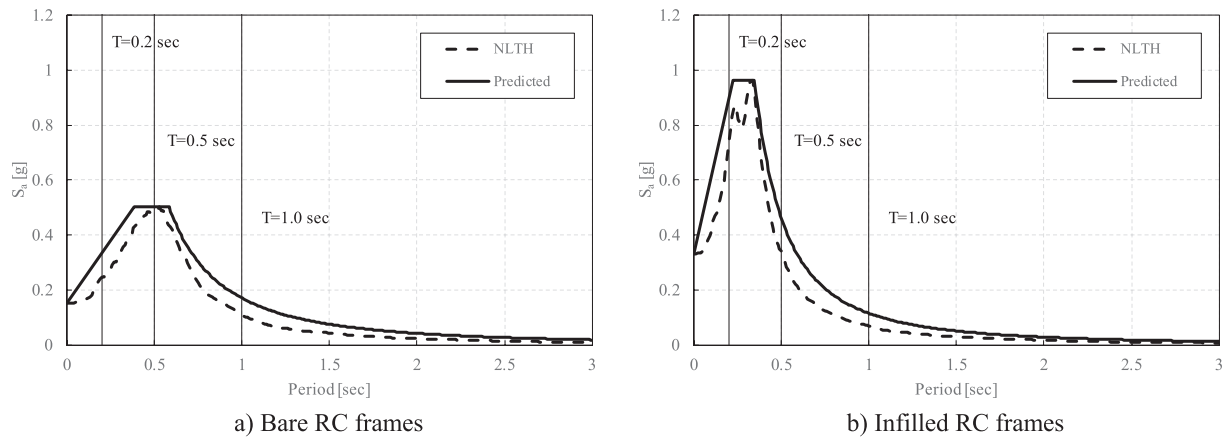


Fig. 13. Comparison between the predicted acceleration top floor response spectra and the median acceleration top floor response spectra obtained from the NLTHAs for low-rise RC frames.

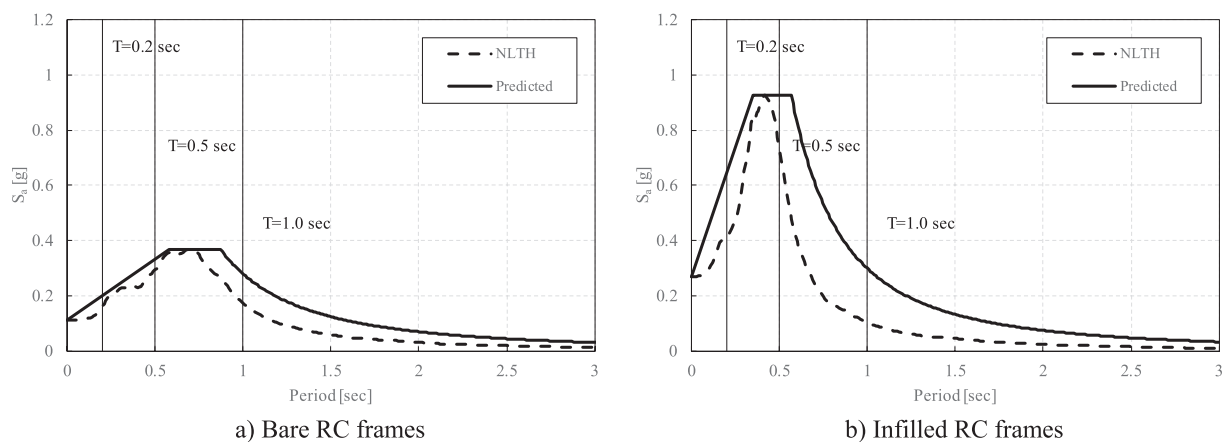


Fig. 14. Comparison between the predicted acceleration floor response spectra and the median acceleration floor response spectra obtained from the NLTHAs for medium-rise RC frames.

preferred to refer to floor absolute acceleration floor response spectra.

The proposed seismic demand models represent a simple example of how the evaluation of the seismic demand at which the non-structural elements are subjected could be improved for regional scale applications. In particular, if the HAZUS methodology is adopted, the proposed seismic models could be used to predict the losses related to the non-structural elements located at the upper floors of low-rise and medium-rise bare and infilled RC moment resisting frames. Similar models could be developed to assess the seismic demand for non-structural elements in high rise-buildings or located at, or near, the ground floor.

## 6. Conclusions

Loss estimation studies, both at the single and regional scale, pointed out that a significant portion of the observed earthquake related losses can be attributed to the damage to non-structural elements, in particular for low seismic intensities. The prediction of non-structural losses requires an accurate evaluation of the seismic demand on non-structural elements. The influence of masonry infills on absolute acceleration floor response spectra and relative displacement floor response spectra in reinforced concrete (RC) buildings subjected to frequent (serviceability level) earthquakes was investigated in this study. The effect of masonry infills on floor response spectra was investigated focusing on a population of 100 RC frames located in a medium-high seismic region in Italy. The floor response spectra were derived following a probabilistic framework such that useful trends could be observed, for both individual and regional scale loss estimations. The

main findings of the study are listed below:

1. The fundamental periods of RC frames are significantly shortened when masonry infills are taken into account. For the building archetypes considered, the percentage in reduction of the fundamental period due to the infill effects varied between 19% and 49%.
2. The results of the NLTHAs demonstrated that the masonry infills significantly affects floor response spectra, in particular if the structure behaves elastically under serviceability level ground motions.
3. The presence of the masonry infills causes a shift of the absolute acceleration floor response spectra peaks to shorter periods and gives rise to a significant amplification of the corresponding peak spectral accelerations.
4. The presence of the masonry infills causes a shift of the relative displacement floor response spectra peaks to shorter periods and modifies the amplitude of the peak spectral displacement. The relative spectral displacements are generally reduced in infilled frames, but no particular trend could be identified. From the obtained results, it was observed that the main parameter governing the difference in the spectral displacement amplitudes is the square of the bare to infilled frame fundamental period ratio.
5. The methodologies currently available in the literature for regional scale loss estimations significantly underestimates the seismic demand on acceleration-sensitive non-structural elements RC frames, both with and without taking into account the influence of the masonry infills.

6. A simple procedure, based on the calibration/fitting of three parameters, have been proposed in order to construct median absolute acceleration floor response spectra from ground response spectra in order to improve the prediction of the seismic demand on acceleration-sensitive non-structural elements at the regional scale. The prediction capability of the proposed procedure was compared with that of the methodologies that are actually used for loss estimation studies at the regional scale. The comparison demonstrated a significant improvement in the prediction of the seismic demand on acceleration-sensitive non-structural elements. However, this proposed approach requires the recalibration of non-structural fragility functions in which probabilities of exceeding given damage states would need to be expressed in terms of spectral accelerations at the fundamental period of the non-structural elements.

The results presented in this study indicates also how further efforts are required to improve the prediction capabilities of regional scale risk models, particularly for evaluating non-structural losses. The modeling assumptions that analysts make both for the skeletal frame (e.g. spread vs. lumped plasticity approaches) as well as for the infills (e.g. triple-strut vs. double-strut vs. single-strut models) could significantly affect the evaluation of the seismic demand, and the same applies to the uncertainties in the infills and how the latter are propagated. Further analyses are required to investigate the influence of specific aspects related to the masonry infills, such as their geometrical and mechanical properties, effect of openings and irregular distribution of the panels. These parameters, which could be treated either in deterministic or probabilistic fashion (modelling them as further random variables in the latter case), are expected to affect both local and global behavior, in particular at higher seismic intensities. The present study provides only a first attempt to improve the prediction of the seismic demand on non-structural elements at the regional scale.

#### Declaration of Competing Interest

The authors declared that there is no conflict of interest.

#### Acknowledgements

The work presented in this paper has been developed within the framework of the project “Dipartimenti di Eccellenza”, funded by the Italian Ministry of University and Research at the University School for Advanced Studied IUSS Pavia.

#### Appendix A. Supplementary material

Supplementary data to this article can be found online at <https://doi.org/10.1016/j.engstruct.2019.109842>.

#### References

- [1] Perrone D, Calvi PM, Nascimbene R, Fischer EC, Magliulo G. Seismic performance of non-structural elements during the 2016 central Italy earthquake. *Bull Earthquake Eng* 2018. <https://doi.org/10.1007/s10518-018-0361-5>.
- [2] O'Reilly GJ, Perrone D, Fox M, Monteiro R, Filiatrault A. Seismic assessment and loss estimation of existing school buildings in Italy. *Eng Struct* 2018;168(1):142–62.
- [3] Villaverde R. Seismic design of secondary structures: state of the art. *J Struct Eng* 1997;123(8):1011–9.
- [4] Miranda E, Taghavi S. Estimation of Seismic Demands on Acceleration-sensitive Nonstructural Components in Critical Facilities, Proceedings of the Seminar on Seismic Design, Performance, and Retrofit of Nonstructural Components in Critical Facilities, ATC 29–2, Newport Beach, CA, 347–360 2003.
- [5] Miranda E, Mosqueda G, Retamales R, Pekcan G. Performance of nonstructural components during the 27 February 2010 Chile Earthquake. *Earthquake Spectra* 2012;28(S1):S453–71.
- [6] Ricci P, De Luca F, Verderame GM. L'Aquila earthquake, Italy: reinforced concrete building performance. *Bull Earthq Eng* 2011;8:285–305.
- [7] Belleri A, Brunesi E, Nascimbene R, Pagani M, Riva P. Seismic performance of precast industrial facilities following major earthquakes in the Italian territory. *J Performance Construct Facilit ASCE* 2015;29(5):04014135.
- [8] Salvatore W, Caprili S, Barberi V. Rapporto dei danni provocati dall'evento sismico del 6 Aprile sugli edifici scolastici del centro storico dell'Aquila, available online: <http://www.reluit.it/>; 2009.
- [9] Welch DP, Sullivan TJ, Calvi GM. Developing direct displacement-based procedures for simplified loss assessment in performance-based earthquake engineering. *J Earthquake Eng* 2014;18(2):290–322.
- [10] FEMA P-58, Seismic Performance Assessment of Buildings, Federal Emergency Management Agency, Washington, DC, 2012.
- [11] FEMA 2012. Multi-hazard loss estimation methodology: HAZUS - MH 2.1 Technical Manual. Washington.
- [12] CEN, Eurocode 8 – Design provisions for earthquake resistant structures, EN-1998-1:2004, Comite Europeen de Normalization, Brussels, Belgium.
- [13] ASCE, Minimum design loads for buildings and other structures, ASCE/SEI Standard 7-10, American Society of civil engineers, Reston.
- [14] Petrone C, Magliulo G, Manfredi G. Seismic demand on light acceleration-sensitive nonstructural components in European reinforced concrete buildings. *Earthquake Eng Struct Dyn* 2015;8(10):1203–17.
- [15] Vukobratovic V, Fajfar P. A method for the direct estimation of floor acceleration spectra for elastic and inelastic MDOF structures. *Earthquake Eng Struct Dyn* 2016;45(15):2495–511.
- [16] Sullivan TJ, Calvi PM, Nascimbene R. Towards improved floor spectra estimates for seismic design. *Earthquakes Struct* 2013;4(1):109–32.
- [17] Calvi PM, Sullivan TJ. Estimating floor spectra in multiple degree of freedom systems. *Earthquake Struct* 2014;7(1):17–38.
- [18] Merino Vela RJ, Brunesi E, Nascimbene R. Derivation of floor acceleration spectra for an industrial liquid tank supporting structure with braced frame systems. *Eng Struct* 2018;171:105–22.
- [19] Welch DP, Sullivan TJ. Illustrating a new possibility for the estimation of floor spectra in nonlinear multi-degree of freedom systems, 16th World Conference on Earthquake Engineering, Santiago, Chile, 9-13 January 2017, Paper N°2632.
- [20] Calvi PM. Relative displacement floor spectra for seismic design of non structural elements. *J Earthquake Eng* 2014;18(7):1037–59.
- [21] Filiatrault A, Perrone D, Merino R, Calvi GM. Performance-Based Seismic Design of Non-Structural Building Elements. *J Earthquake Eng* 2018. <https://doi.org/10.1080/13632469.2018.1512910>.
- [22] Ricci P, Verderame GM, Manfredi G. Analytical investigation of elastic period of infilled RC MRF buildings. *Eng Struct* 2011;33(2):308–19.
- [23] Perrone D, Leone M, Aiello MA. Evaluation of the Infill Influence on the elastic period of existing RC frames. *Eng Struct* 2016;123:419–33.
- [24] Ricci P, Di Domenico M, Verderame GM. Empirical-based out-of-plane URM infill wall model accounting for the interaction with in-plane demand. *Earthquake Eng Struct Dyn* 2017;47(3):802–27.
- [25] Morandi P, Hak S, Magenes G. Experimental and numerical seismic performance of strong clay masonry infills. *Research Report Eucentre* 2017/02.
- [26] Di Meo A, Borzi B, Faravelli M, Pagano M, Ceresa P, Monteiro R, et al. Seismic vulnerability assessment of the urban building environment in Nablus Palestina. *Int J Architec Heritage* 2018;12(7–8):1196–215.
- [27] Villar-Vega M, Silva V, Crowley H, Yepes C, Tarque N, Acevedo AB, et al. Development of a fragility model for the residential building stock in South America. *Earthquake Spectra* 2017;33(2):581–604.
- [28] Cavaleri L, Di Trapani F. Cyclic response of masonry infilled RC frames: Experimental results and simplified modeling. *Soil Dyn Earthquake Eng* 2014;65:224–42.
- [29] Sassun K, Sullivan TJ, Morandi P, Cardone D. Characterising the in-Plane Seismic Performance of Infill Masonry. *Bull New Zeal Soc Earthq Eng* 2016;49:100–17.
- [30] De Luca F, Morciano E, Perrone D, Aiello MA. MID1.0: masonry infilled rc frame experimental database. In: di Prisco M, Menegotto M, editors. Proceedings of Italian Concrete Days 2016. ICD 2016. Lecture Notes in Civil Engineering. Cham: Springer; 2016.
- [31] Sousa L, Monteiro R. Seismic retrofit options for non-structural building partition walls: Impact on loss estimation and cost-benefit analysis. *Eng Struct* 2018;8:27.
- [32] Dolšek M, Fajfar P. The effect of masonry infills on the seismic response of a four-story reinforced concrete frame: a deterministic assessment. *Eng Struct* 2008;30:1991–2001.
- [33] Perrone D, Leone M, Aiello MA. Non-linear behavior of masonry infilled RC frames: influence of masonry mechanical properties. *Eng Struct* 2017;150:875–91.
- [34] Lucchini A, Mollaioli F, Bazzurro P. Floor response spectra for bare and infilled reinforced concrete frames. *J Earthquake Eng* 2014;18(7):1060–82.
- [35] Surana M, Pisode M, Singh Y, Lang DH. Effect of URM infills on inelastic floor response of RC frame buildings. *Eng Struct* 2018;175:861–78.
- [36] Amanat KM, Hoque E. A rationale for determining the natural period of RC building frames having infill. *Eng Struct* 2006;28(4):495–502.
- [37] Crowley H, Pinho R. Period-height relationship for existing european reinforced concrete buildings. *J Earthquake Eng* 2004;8(1):93–119.
- [38] Borzi B, Pinho R, Crowley H. Simplified pushover-based vulnerability analysis for large-scale assessment of RC buildings. *Eng Struct* 2008;30:804–20.
- [39] Brunesi E, Parisi F. Progressive collapse fragility models of European reinforced concrete framed buildings based on pushdown analysis. *Eng Struct* 2017;152:579–96.
- [40] Rossetto T, Elnashai A. A new analytical procedure for the derivation of displacement-based vulnerability curves for populations of RC structures. *Eng Struct* 2005;27:397–409.
- [41] Mazzoni S, McKenna F, Scott MH. Fenves GL. OpenSees Command language manual. Pacific Earthquake Eng Res (PEER) Center 2006.
- [42] Spaone E, Filiippou FC, Taucer FF. Fibre beam-column model for non-linear analysis of RC frames: Part 1 Formulation. *Earthquake Eng Struct Dynamics*

- 1996;25:711–25.
- [43] Chang GA, Mander JB. Seismic Energy Based Fatigue Damage Analysis of Bridge Columns: Part 1 – Evaluation of Seismic Capacity. NCEER Technical Report No. NCEER-94-0006 State University of New York, Buffalo, N.Y.
- [44] Mainstone RJ. On the stiffnesses and strengths of infilled frames. *Proc Inst Civ Eng* 1971;49(2).
- [45] Stafford Smith B, Carter C. A method of analysis for infilled frames. *Proc Inst Civ Eng* 1969;44(1):31–48. <https://doi.org/10.1680/iicep.1969.7290>.
- [46] PEER NGA-West database, available on-line: <http://peer.berkeley.edu/ngawest>.
- [47] Stucchi M, Meletti C, Montaldo V, Crowley H, Calvi GM, Boschi E. Seismic hazard assessment (2003–2009) for the Italian building code. *Bull Seismol Soc Am* 2011;101(4):1885–911. <https://doi.org/10.1785/0120100130>.
- [48] NTC08. Nuove norme tecniche per le costruzioni. D.M. Infrastrutture: 2008.
- [49] Jayaram N, Lin T, Baker JW. A computationally efficient ground-motion selection algorithm for matching a target response spectrum mean and variance. *Earthquake Spectra* 2011;27(3):797–815.
- [50] Iervolino I, Chioccarelli E, Cito P. REASSESS V1.0: A computationally efficient software for probabilistic seismic hazard analysis. ECCOMAS Congress 2016: VII European on Computational Methods in Applied Sciences and Engineering. In: M. Papadrakakis, V. Papadopoulos, G. Stefanou, V. Plevris, Crete Island, Greece, 5–10 June 2016.
- [51] Baker JW, Jayaram N. Correlation of spectral acceleration values from NGA ground motion models. *Earthquake Spectra* 2008;24(1):299–317.
- [52] Filiatrault A, Tremblay R, Christopoulos C, Folz B, Pettinga D. Elements of earthquake engineering and structural dynamics. 3rd Edition Montreal, Canada: Polytechnic International Press; 2013. p. 874.